JMEPEG (2010) 19:1031–1036
DOI: 10.1007/s11665-009-9567-7

1059-9495/$19.00

Investigations of White Layer Formation During Machining of Powder Metallurgical Ni-Based ME 16 Superalloy

S.C. Veldhuis, G.K. Dosbaeva, A. Elfizy, G.S. Fox-Rabinovich, and T. Wagg

(Submitted April 2, 2009; in revised form August 19, 2009)

Surface integrity of machined parts made from the advanced Ni-based superalloys is important for modern manufacturing in the aerospace industry. Metallographic observations of the ME 16 alloy microstructure were made using optical metallography and a high-resolution scanning electron microscope with energy dispersive x-ray spectrometer (HR SEM/EDS). Tool life of cemented carbide inserts with TiAlN coating during machining (finishing turning operation) of ME 16 superalloy has been studied and wear patterns of the cutting tools were identified. Surface integrity of the machined part after completion of the turning operation was investigated. The morphology of machined parts has been examined and cross-sections of the machined surfaces have been analyzed. The formation of white layer on the surface of the machined part was studied for varied machining conditions. It was found that a 2-4 μm thick white layer forms during turning of the ME 16 superalloy. This layer was investigated using EDS and XRD. The studies show that the white layer is an oxygen-containing layer with a high amount of aluminum, enriched by chromium and tungsten. Under specific cutting conditions, the structure of white layer transforms into a γ-alumina. Formation of this thermal barrier ceramic white layer on the surface of the machined part negatively affects its surface integrity and cutting tool life.

Keywords aerospace, machining, metallography, superalloys

1. Introduction

Fine grain ME 16 nickel base superalloy forgings are produced by powder metallurgy processing (PM) for aerospace applications (Ref 1). ME 16 has been recently developed for turbine and disk applications requiring strength and creep resistance at relatively high temperatures (600-800 °C), as well as well as resistance to fatigue crack initiation at the lower temperatures (300-600 °C) (Ref 2). Generally, PM superalloys having increased processability will meet increased temperature capability while maintaining strength and lower density (Ref 3).

Two major advantages accrue from making a powder metallurgy alloy, due to the rapid solidification rates of atomized metal droplets. The grain size of the product is very small, of the order of microns, much smaller than in typical cast materials (Ref 3, 4). Because of lack of segregations or precipitations, powder metallurgy aerospace alloys can be designed or tailored to contain a higher alloy content than is possible using casting techniques. This, in turn, should contribute to the development of alloys with still greater strength. Also, a more uniform structure compared to cast materials gives a better, more homogeneous distribution of the strengthening phases throughout the powder compact and should result in better properties (Ref 4, 5).

Machining of advanced ME 16 alloy is a significant challenge. This is due to a more complex combination of material properties, including lowering of thermal conductivity that leads to elevating temperatures at the tool/chip interface during cutting, work hardening tendency during machining that becomes more severe with increased strengthening of this alloy, and intensive adhesion to the surface of the tooling under operation. Tool life can be significantly decreased (Ref 5, 6). Generally, PM microstructure improvements such as absence of large carbide particles have been accompanied by decreased sensitivities to defects during machining (Ref 7, 8). On the other hand, one of the key requirements for rotor blades and discs superalloys is fatigue strength (Ref 3). In order to maintain fatigue strength, the most challenging aspects when machining these materials come from the workpiece surface quality point of view. For instance, formation of the white layer poses a significant potential danger to fatigue life (Ref 9). For this material to be used in critical engine components, this issue must be resolved first.

To date there is not much information available on the machining of ME 16. This paper focuses on investigations of structural characteristics of ME 16 alloy and surface integrity issues of the machined part, with an emphasis on the features of the white layer formation.

S.C. Veldhuis, G.K. Dosbaeva, G.S. Fox-Rabinovich, and **T. Wagg**, Department of Mechanical Engineering, McMaster University, 1280 Main St. W., Hamilton, ON L8S 4L7, Canada; and **A. Elfizy,** Manufacturing Engineering Development, Pratt & Whitney Canada, 1000 Marie-Victorin, Longueuil, QC J4G 1A1, Canada. Contact e-mail: dosby@mcmaster.ca.

Table 1 ME 16 alloy elemental composition wt.% based on the quantitative EDS data

Elemental content							
Al	**Ti**	**Cr**	**Co**	**W**	**Ta**	**Mo**	**Nb**
3.1	2.6	10.4	20.5	3.0	1.4	1.3	1.4

Balance is minor amount of nickel and alloying elements

2. Experimental

In this work, the structure and machinability of the powder metallurgical nickel-based superalloy ME 16 has been studied in detail. Intensive studies of the ME 16 alloy microstructure, surface morphology of the machined part and the white layer formation have been performed using various methods including optical metallography, x-ray diffraction (XRD) and a high-resolution scanning electron microscope with energy dispersive

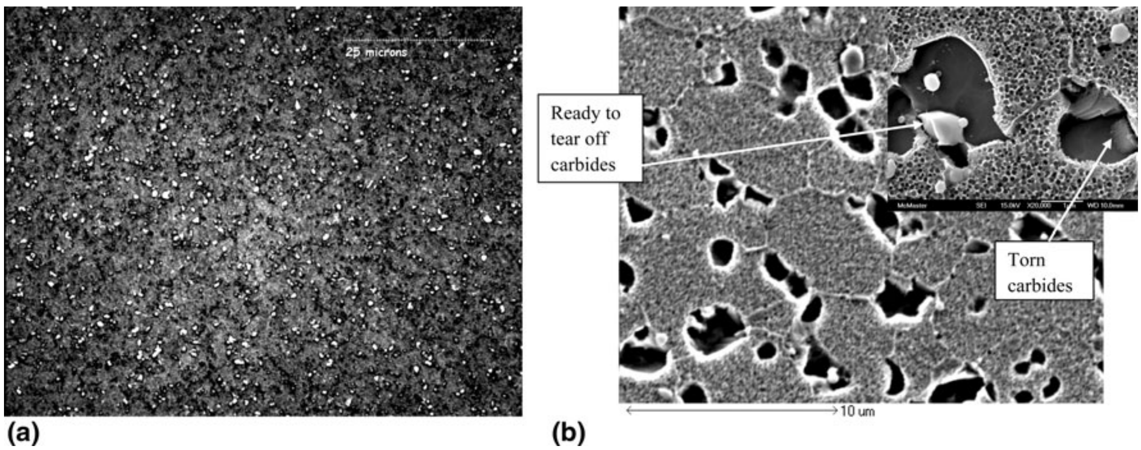

Fig. 1 Optical and SEM metallography of ME 16 alloy (workpiece material): (a) optical image, magnification 1600×; (b) HR SEM image, magnification 5000× and 20000×

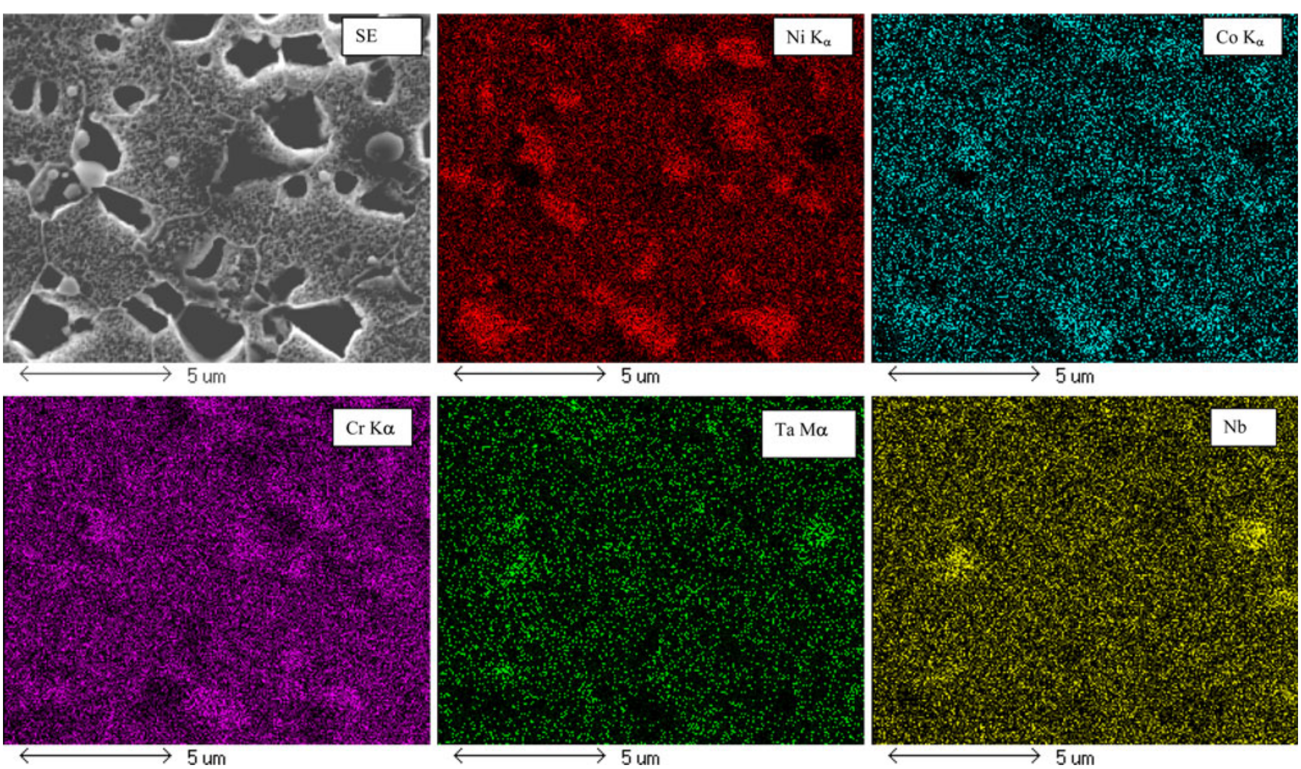

Fig. 2 SEM elemental map of ME 16 alloy. TaC and NbC formation

x-ray spectrometer (HR SEM/EDS). The machining experiments were performed using a Boehringer VDF 180 turning Centre. Tool life was studied under various cutting speed conditions. The tool life was evaluated as a length of cut (m) when flank wear of cutting insert reaches 300 μm. The parameters of cutting used during turning experiments (finishing operation) were the following: speed 30-65 m/min, depth of cut 0.125 mm, feed 0.1225 mm/rev. Commercial cemented carbide WC-Co inserts (K-grade) with TiAlN PVD coating, commonly used for cutting of Inconel alloys, were employed in this work. All the cutting tests were performed under wet machining conditions using Commonwealth water-based coolant CommCool Max.

Surface roughness measurements were carried out with a surface roughness tester, Zygo New View 5000 interferometer optical profiling system, using evaluation and cut-off lengths of 5 and 0.8 mm, respectively. The surface roughness was taken at four locations (90° apart) and repeated twice at each point on the face of the machined surface and the average values were reported.

3. Results and Discussion

3.1 Study of the Microstructure and Properties

The general elemental composition of the ME 16 sample is presented in Table 1. Figure 1 presents optical metallographic images of the ME 16 alloy. There are evenly distributed fine-grained carbides in the structure (Fig. 1a). These carbides have low cohesion to the matrix (Fig. 1b) and were found to be easily torn off during sample preparation (polishing and etching). They have a complex composition. The matrix of ME 16 is extremely fine grained with an average grain size of 7 μm (fine grains of Ni-based γ-phase, Fig. 1b). Figure 2 shows the EDS elemental map for ME 16 alloy. The ME 16 alloy contains fine (microns-sized) carbides, mainly (Ta, Ti, Nb) C, within a ductile (Co, Ni, Cr) matrix phase (Ref 10). The hardness of ME 16 alloy was measured and compared to the widely used Inconel 718 Ni-based superalloy. Hardness of both alloys is similar: HRC 47-48 for the Inconel 718 and 46-47 for the ME 16.

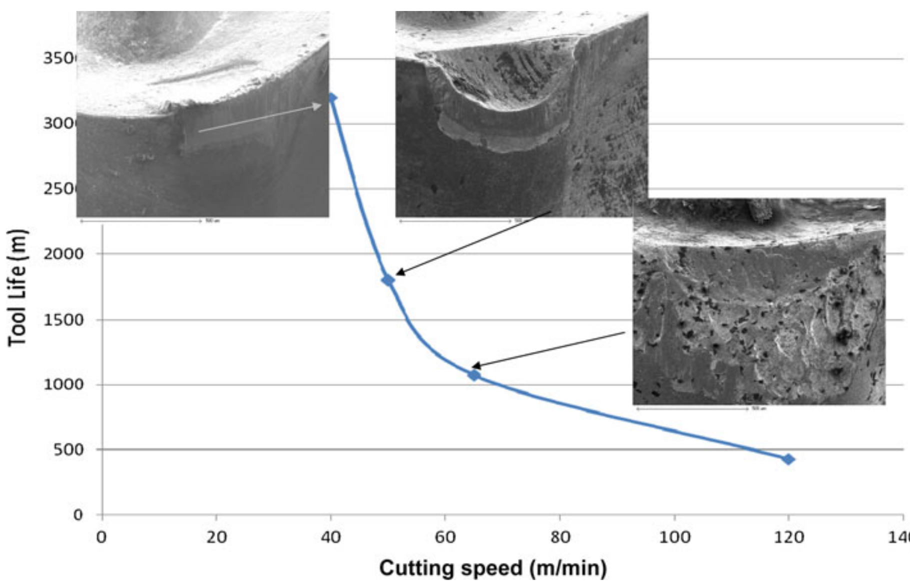

Fig. 3 Tool life and crater formation of CC inserts with TiAlN coating vs. cutting speed during machining of ME 16 alloy

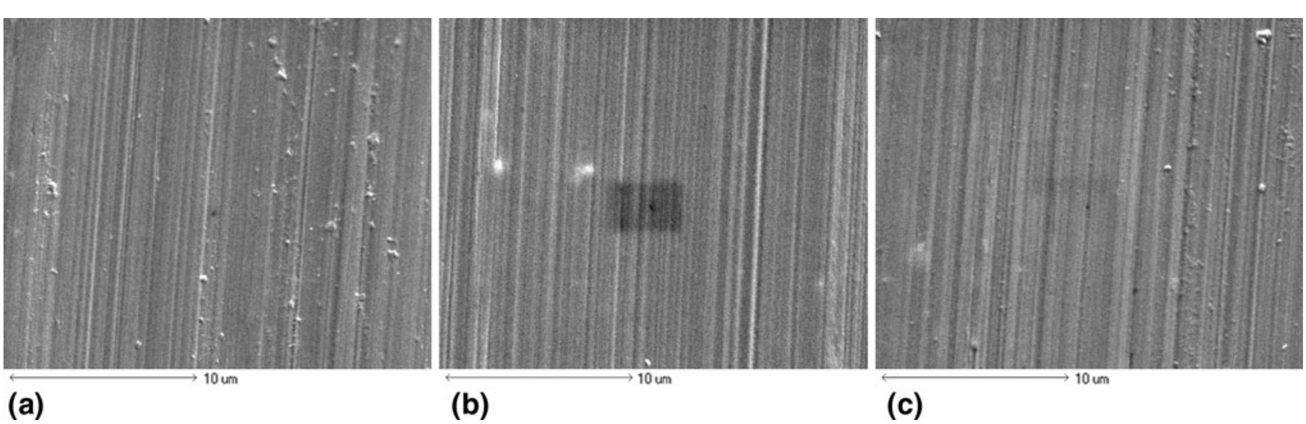

Fig. 4 Surface finish of ME 16 at various cutting speeds: (a) 30 m/min, (b) 40 m/min, and (c) 50 m/min. Magnification 5000×

3.2 Tool Life and Wear Behavior Studies

The tool life of cemented carbide inserts with TiAlN coating versus cutting speed is presented in Fig. 3. Tool life notably decreased with increasing cutting speeds from 20 to 65 m/min. Wear patterns were studied for the coated cemented carbide inserts. Figure 3 presents SEM images of worn cemented carbide inserts. Cratering of the rake surface was observed to be significant and increased rapidly with a rise in cutting speed. The cratering was found to be quite severe at 50 m/min and it was catastrophic at 65 m/min. This severe diffusive wear can be caused by high temperatures at the rake surface, which is most likely due to the low thermal conductivity of the ME 16.

3.3 Surface Integrity Studies

The surface morphology of the machined part made of ME 16 alloy is presented in Fig. 4(a)-(c). No visible defects were detected on the surface. Surface roughness data show that the average roughness R_a after turning experiments (finishing operation) are almost similar: 2.535, 2.707, and 2.668 μm correspondingly.

However, metallographic sections showed the machining of the ME 16 super alloy using cemented carbide inserts with TiAlN coating results in the formation of a white layer under varying cutting conditions. At speeds of 30 and 40 m/min, the white layer is thick and noncontinuous (Fig. 5a, b) and its average thickness is 4 μm. At 50 m/min, the layer is continuous and its thickness is diminished down to 2 μm (Fig. 5c). The EDS point analysis shows that the white layer is a metal-ceramic compound (Al-Cr-O) that forms on the surface during machining (Fig. 5). EDS elemental map confirm data of point EDS analysis and also indicates aluminum and tungsten in this layer (Fig. 6). This layer has poor adhesion to the substrate. It is almost flaked off in Fig. 5 and 6.

XRD studies of the white layer formed on the surface of machined part indicate the formation of a γ-alumina phase (see corresponding spectrum in Fig. 7a) at cutting speed of 50 m/min. The γ-alumina is a low-temperature modification of α-alumina (Ref 11, 12) and its formation indicates that the actual temperatures in the cutting zone are around 750-800 °C. However γ-alumina has similar characteristics to the α-alumina and has a similar effect on the surface integrity of the machined part. This undesirable phase cannot be detected by XRD at the lower cutting speeds of 40 m/min (Fig. 7b).

Alumina phase found in the white layer is ceramic and acts as a thermal resistant layer that is formed in situ during cutting on the machined surface of the ME 16 alloy. A significant portion of the heat generated during cutting goes into the tool instead of workpiece. These aspects may have encouraged intensive cratering on the rake surface of the cutting tool (Fig. 3). In addition, the ceramic layer is extremely brittle compared to the core. The machined part with this layer could have reduced cycle fatigue strength due to high possibility of crack formation within the white layer (Ref 13).

The microhardness distribution for the machined surface of ME 16 at the cutting speeds is presented in Fig. 8. The data presented show that at cutting speeds above 40 m/min a softening of a region close to the surface layer takes place. This is related to the hardness of the workpiece material layer below the superficial (2-4 μm thick), white layer (Fig. 5). White layer composed of ceramic alumina phase may prevent heat from being evenly absorbed by the core of the machined part (Ref 14, 15). This could worsen cutting conditions at the higher cutting speed.

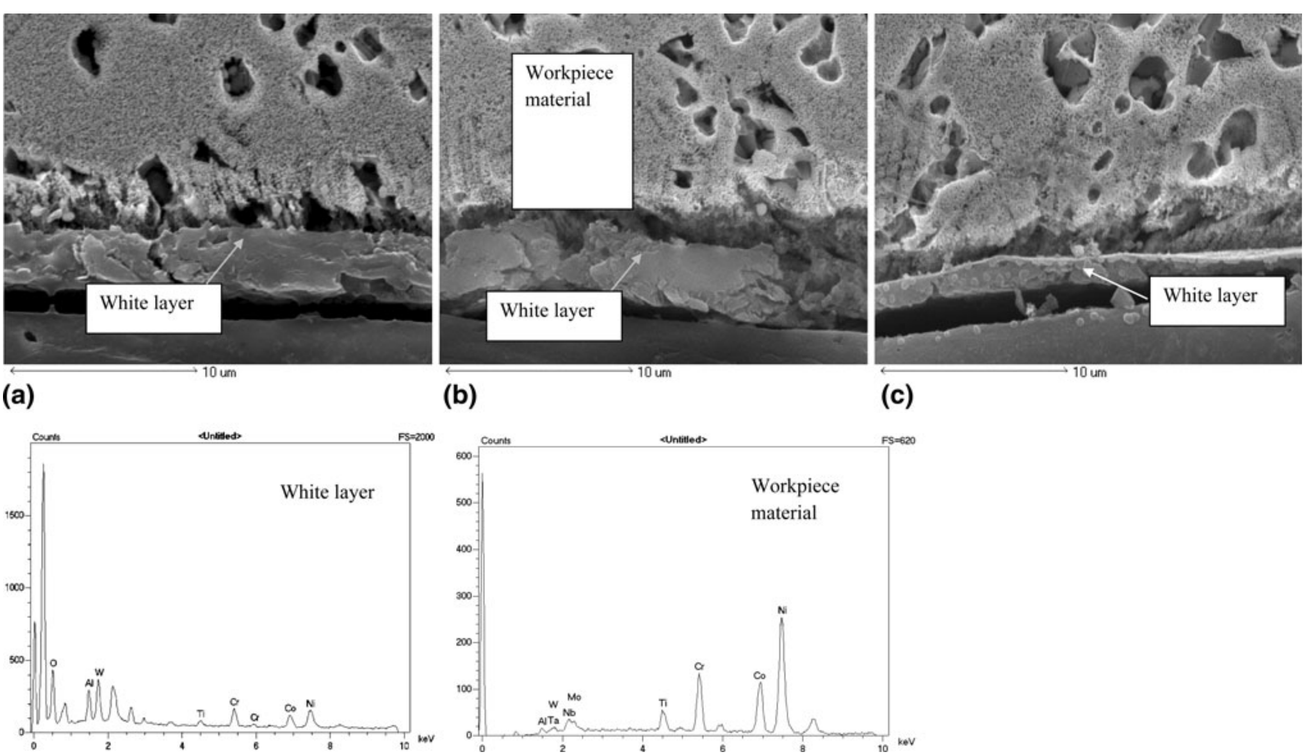

Fig. 5 SEM images and EDS analyses of cross-sections of machined part made of ME 16 alloy, 5000×. White layer, formed at cutting speed: (a) 30 m/min, (b) 40 m/min, and (c) 50 m/min

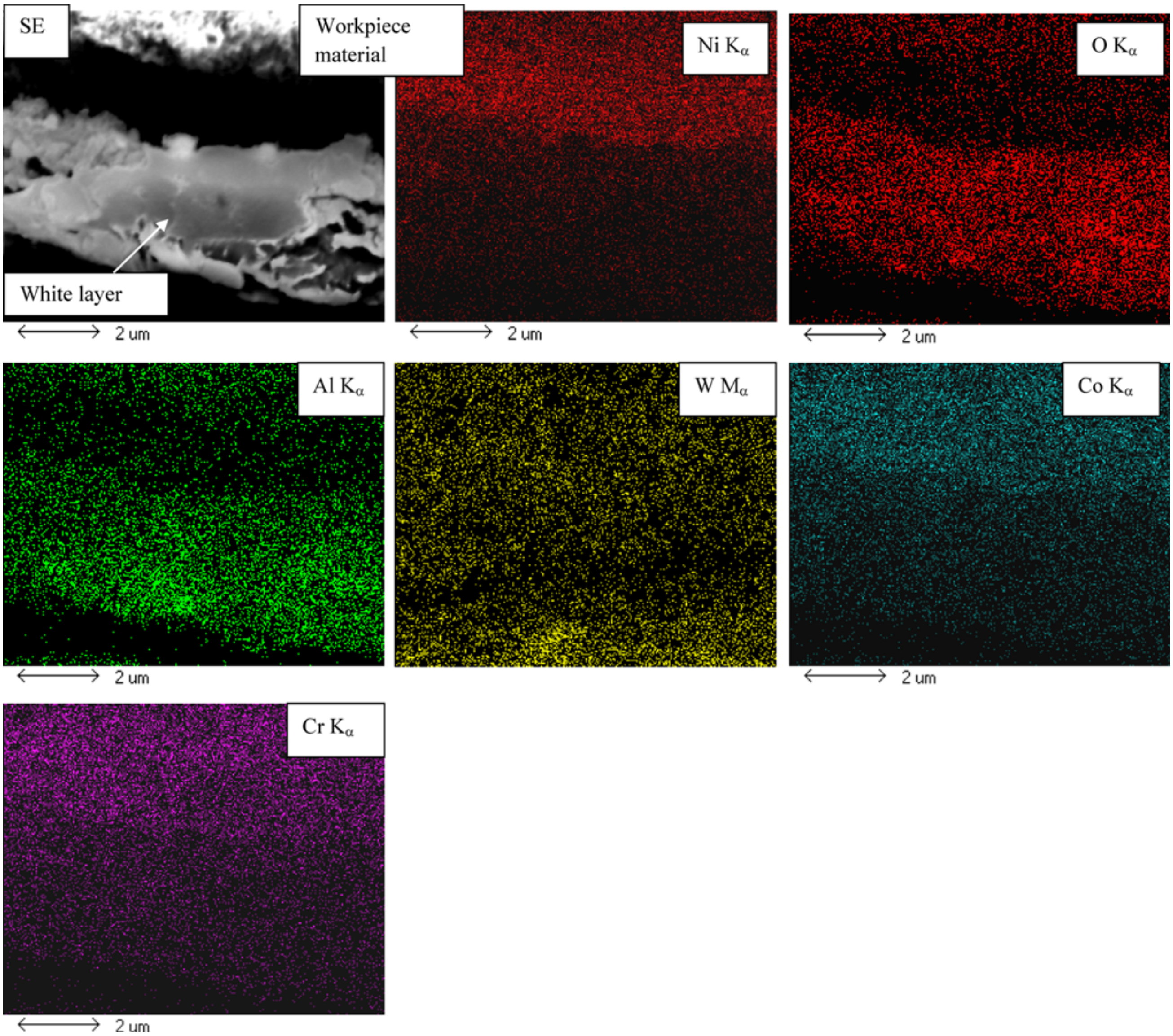

Fig. 6 Elemental map of the white layer on the surface of machined part of ME 16 alloy. Cutting speed 40 m/min

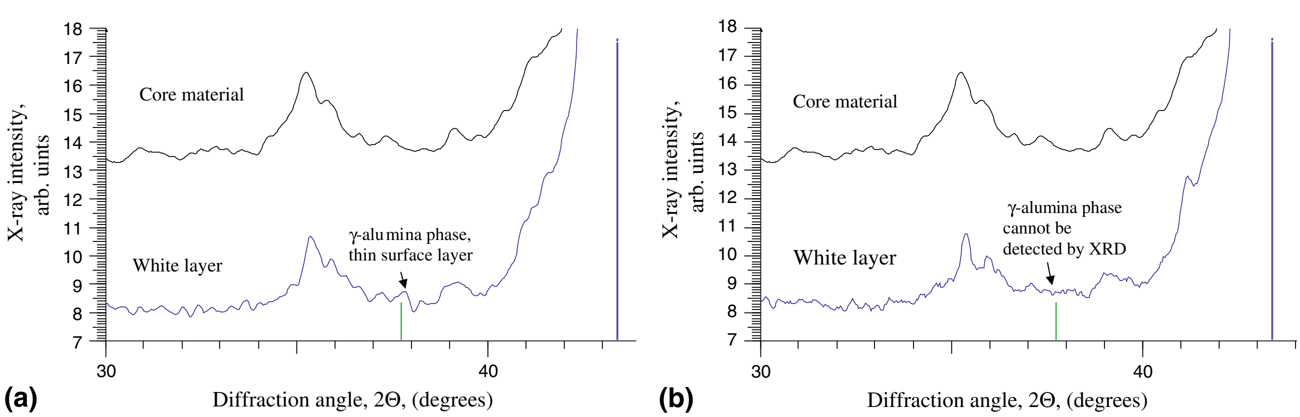

Fig. 7 XRD spectra of white layer and workpiece material for machined surface of ME 16 alloy. Cutting speed: (a) 50 m/min and (b) 40 m/min

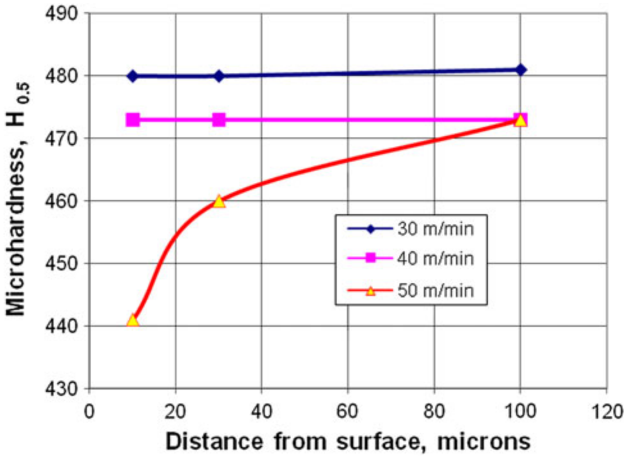

Fig. 8 Microhardness distribution on the surface of machined part made of ME 16 alloy. Cutting speed 30-50 m/min

4. Conclusions

Investigations of the tool life and surface integrity of the machined part made of Ni-based ME 16 alloy show that machining by a finishing turning operation of ME 16 alloy results in a 2-4 μm thick white layer formation on the machined surface, depending on the machining conditions. This layer contains oxygen with a high amount of aluminum, enriched by chromium and tungsten. Under specific cutting conditions, the structure of the white layer transforms into γ-alumina. This ceramic layer is thermally resistant, brittle, and abrasive. Due to the formation of the thermal barrier alumina-content white layer, the heat generated during cutting may not be evenly absorbed by the core of workpiece material. This could negatively affect surface integrity of the machined parts and cutting tool life at the higher cutting speed.

Acknowledgment

This research was funded by Pratt & Whitney Canada.

References

1. Superalloy Optimized for High-Temperature Performance in High-Pressure Turbine Disks, U.S. Patent 6,521,175, 2 Nov 2003
2. Nickel Based Superalloy Compositions, Articles, and Methods of Manufacture, EP Patent 1,710,322 A1, 11 Oct 2006
3. J. Gayda and T.P. Gabb, Fatigue Behavior of a Third Generation PM Disk Superalloy, NASA/TM—2008-215462, Glenn Research Center, Cleveland, OH, 2008
4. G.D. Smith, Future Trends in Key Nickel Alloy Markets, *JOM*, 2006, **58**(9), p 38
5. R. Arunachalam and M.A. Mannan, Machinability of Nickel-Based High Temperature Alloys, *Mach. Sci. Technol.*, 2000, **4**(1), p 127–168
6. L. Settineri and R. Levi, Surface Properties and Performance of Multilayer Coated Tools in Turning Inconel, *CIRP Ann.*, 2005, **54**(1), p 515–518
7. D.A. Axinte, P. Andrews, W. Li, N. Gindy, and P.J. Withers, Turning of Advanced Ni Based Alloys Obtained via Powder Metallurgy Route, *CIRP Ann.*, 2006, **55**(1), p 117–120
8. T.P. Gabb, J. Telesman, P.T. Kantzos, P.J. Bonacuse, R.L. Barrie, and D.J. Hornbach, Stress Relaxation in Powder Metallurgy Superalloy Disks, *TMS Lett.*, 2004, **1**(5), p 115–116
9. G. Boothroyd and W.A. Knight, *Fundamentals of Machining and Machine Tools*, CRC Press, Boca Raton, 2006
10. P.T. Gabb, A. Garg, D.L. Ellis, and M.K. O'Connor, Detailed Microstructural Characterization of the Disk Alloy ME3, NASA/TM-2004-213066, NASA, Washington, DC, 2004
11. P.S. Sklad, C.J. McHargue, C.W. White, and G.C. Farlow, *High Tech Ceramic*, P. Vincenzini, Ed., Elsevier, Amsterdam, 1987, p 1073
12. C.W. White, L.A. Boatner, P.S. Sklad, C.J. McHargue, J. Rankin, G.C. Farlow, and M.J. Aziz, Ion Implantation and Annealing of Crystalline Oxides and Ceramic Materials, *Nucl. Instrum. Methods B*, 1988, **32**(11), p 115–116
13. G. Poulachon, A. Albert, M. Schluraff, and I.S. Jawahir, An Experimental Investigation of Work Material Microstructure Effects on White Layer Formation in PCBN Hard Turning, *Int. J. Mach. Tools Manuf.*, 2005, **2**, p 211–218
14. A. Ramesh, S.N. Melkote, L.F. Allard, L. Riester, and T.R. Watkins, Analysis of White Layers Formed in Hard Turning of AISI 52100 Steel, *Mater. Sci. Eng. A*, 2005, **390**, p 88–97
15. J. Vinodh Jose and M.S. Shunmugam, Investigation into White Layer Formed on Wire Electrical Discharge Machined Ti6Al4V Surface, *Int. J. Mach. Mater.*, 2009, **6**(3–4), p 234–249